Investigation of the Interactions of β-Peptides with DNA Duplexes by Circular Dichroism Spectroscopy[1])

by **Kenji Namoto**[2]), **James Gardiner**[3]), **Thierry Kimmerlin**[4]), and **Dieter Seebach***

Laboratorium für Organische Chemie, Departement Chemie und Angewandte Biowissenschaften, Eidgenössische Technische Hochschule, ETH-Zürich, Hönggerberg, HCI, Wolfgang-Pauli-Strasse 10, CH-8093 Zürich
(phone: +41 44 632 2990; fax: +41 44 632 1144; e-mail: seebach@org.chem.ethz.ch)

Dedicated to Professor *Helgard Raubenheimer*, University of Stellenbosch, on the occasion of his 65th birthday.

The interaction of β-peptides with the DNA duplexes of $dA_{20}dT_{20}$ and a GCN4-binding CRE sequence was examined. To gauge the factors that govern these interactions, two β-pentadecapeptides, **1** and **2**, a β-dodecapeptide, **3**, three β-decapeptides, **4**–**6**, three β-heptapeptides, **7**–**9**, and β-octaarginine **10** were designed and synthesized. The β-peptides were conceived to adopt a β-peptide 3_{14} helix, in which the side chains at position *i* and *i*+3 are aligned vertically along one side of the helix. The side chains of Lys, Asn, and Arg were positioned such that potential H-bonding sites were created for a helical conformation to interact with the base pairs of DNA. CD Analysis showed that β-peptides **1**, **2**, and **10** interacted with $dA_{20}dT_{20}$. In addition, β-peptides **1** and **2** showed significant interaction with a DNA-duplex 20mer containing the ATF/CREB recognition sequence for the regulatory protein GCN4. It is impossible, at this stage of the investigation, to make a safe proposal about the actual nature of the interaction of the structures(s) of the complexes, the formation of which is suggested by the CD spectra reported herein.

1. Introduction. – The interaction of peptides and proteins with DNA is fundamental to the chemistry of life [2], and, as such, has dominated the contemporary scene of modern molecular sciences. Crucial processes such as DNA replication, restoration, compaction, transcription, and degradation are all regulated by proteins capable of recognizing, and thereby complexing with, the DNA double helix [3]. Many DNA-binding proteins contain ordered structures that lead to selective recognition and binding of specific DNA sequences. Examples of such structures include the zinc-finger, the leucine zipper, and the helix–turn–helix, terms now familiar in biochemistry and protein

[1]) Part of the results described herein was mentioned in a preliminary communication [1].

[2]) Postdoctoral Fellow at ETH Zürich, 2002–2004, financed by *Novartis Pharma AG* and by the *Swiss National Science Foundation*, Project No. 200-058831.99. Present address: *Novartis Pharma AG*, NIBR, CH-4002 Basel.

[3]) Postdoctoral Fellow at ETH, 2004–2007, financed by the *New Zealand Foundation for Research Science and Technology*, Project No. SWSS0401.

[4]) Part of the ETH dissertation No. 15800. Present address: *Novartis Institutes for Biomedical Research GmbH & Co KG*, A-1235 Vienna.

science when describing protein–DNA interactions [2]. Such interactions can be base-specific when mediated by H-bonds with Asn- or Gln-amide side chains, or sequence-independent where ionic interactions bridge the phosphate backbone of the DNA and the cationic side chains of Arg, Lys, and His residues [3]. Notably, many of the DNA- or RNA-binding sites in these proteins are in the form of protruding loops or α-helices that fit into the major or minor groove of the nucleic acid, with the solution conformation of such binding motifs generally being quite different in the stabilized DNA–ligand complex compared to that of the native ligand [2][3]. In some cases, it is only upon these ligand/DNA-specific interactions that certain binding conformations are stabilized enough to be observed. Of particular interest to us are the α-helical motifs formed upon the interaction of peptide sequences with nucleobases in the major groove of DNA. We previously reported in a preliminary note the interaction of the β^3-pentadecapeptide **1** with DNA duplexes (*Fig. 1*) [1]: CD analysis suggested that **1** adopts a conformation resembling a 3_{14} helix upon complexation with the DNA duplexes $dA_{20}\cdot dT_{20}$ and $dG_{20}\cdot dC_{20}$. It was further demonstrated that the peptide interacts with single-stranded as well as double-stranded DNA. Intrigued by this initial result, we have now prepared additional peptides of varying lengths and substitution patterns with the aim of further understanding the interactions involved in the hitherto unprecedented complexation of β-peptides with DNA[5]).

2. Design of the β-Peptides 2–10. – The concepts behind the design of **1** have been described previously [1]. Namely, that *a*) the peptide can be conceived to adopt a β-peptide 3_{14} helix, in which the side chains at position i and $i+3$ are aligned vertically along one side of the helix (*Fig. 1*), *b*) consequently, three streaks of side chain groups run in parallel along the cylinder of the helix at *ca.* 120° apart from each other [7], and *c*) one of the streaks possesses three Asn residues to possibly engage in a H-bonding interaction. Based on these concepts, and following the preliminary indications of interactions between **1** and oligonucleotides ($dA_{20}dT_{20}$, $dG_{20}dC_{20}$), pentadecamer **2** was designed, in which the Asn side chains of **1** have been replaced by Me groups (β^3hAla), to assess the validity of the concept *c*, namely that Asn residues act as possible H-bond recognition sites. To define the minimum peptide length required for the observed interactions, β-dodecapeptide **3**, and a series of β-deca- and β-heptapeptides, **4**–**9**, were designed, mimicking the residue arrangements of **1** and **2** in one way or another (see the cylindrical representations of each peptide in *Fig. 2*). Dodecapeptide **3** was based on the structure of **2** but with one less turn of the proposed helix. Decapeptide **4** and heptapeptide **7** were based on the structure of **1**, mimicking the positions of Lys and Asn residues. Decapeptides **5** and **6**, and heptapeptide **8**, are close analogs of **2**, again mimicking the positions of Lys side chains. Heptapeptide **9** is an analog of heptapeptide **7** that retains the Asn side chains but lacks those of Lys[6]). In addition, β-

---

[5]) A special type of β-peptide, the oligo-β-arginines, have been shown to enter cells and bind to DNA, probably solely due to charge-charge interactions (*vide infra* and [4–6]).

[6]) The linear arrangement of Lys and Asn side chains of peptides **2**–**6**, and **9**, minus the C-terminal β-Phe, constitute palindromic sequences in that the order and atomic distance between the side chain residues are the same in both directions.

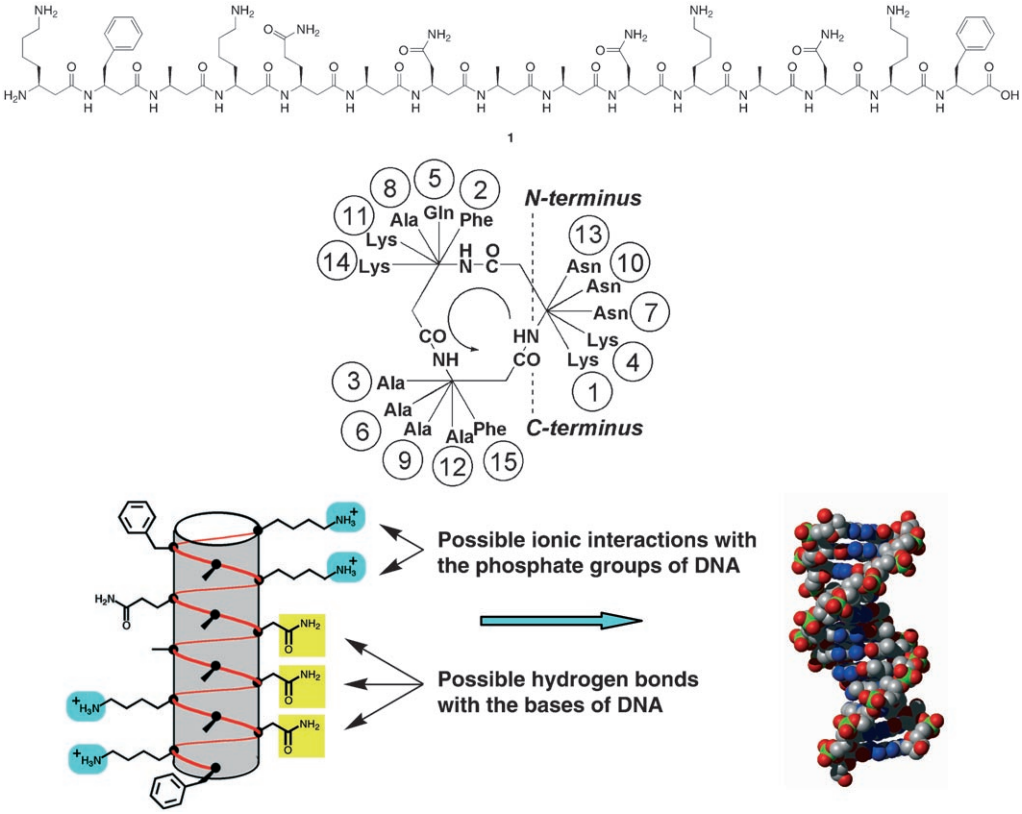

Fig. 1. *Constitutional and configurational formulae, and view along the axis, of an idealized* 3_{14}*-helical structure of* β^3*-pentadecapeptide* **1**, *together with a schematic view of projected interactions with a DNA double helix*

octaarginine **10** was chosen for analysis as this β-peptide[5])[7]) has been shown to permeate the cell membranes of not only living eukaryotic cells but also of *Gram*-positive and *Gram*-negative bacteria, binding strongly to the nuclear material [5][6].

3. Synthesis of β-Peptides 1–10. – In line with previous protocols, β-peptides **1**–**9** were prepared by solid-phase synthesis on *Wang* resin, using standard Fmoc strategy [8]. β-Octaarginine **10** was prepared by fragment coupling on *Rink* amide AM resin according to our previously published procedure [5]. Aliquots of the crude products were purified by preparative RP-HPLC to give 7–10 mg of each of the β-peptides in $>95\%$ purity. The peptides were subsequently characterized by ^{1}H- and ^{13}C-NMR, and MALDI high-resolution mass spectrometry.

---

[7]) One might expect that the repulsion of the positive charges in β-oligoarginines disfavors helical structures and favors other arrangements, such as a fully extended linear conformation. On the other hand, it is indicated by CD spectra that these compounds might indeed fold, at least partially, to helical secondary structures [4].

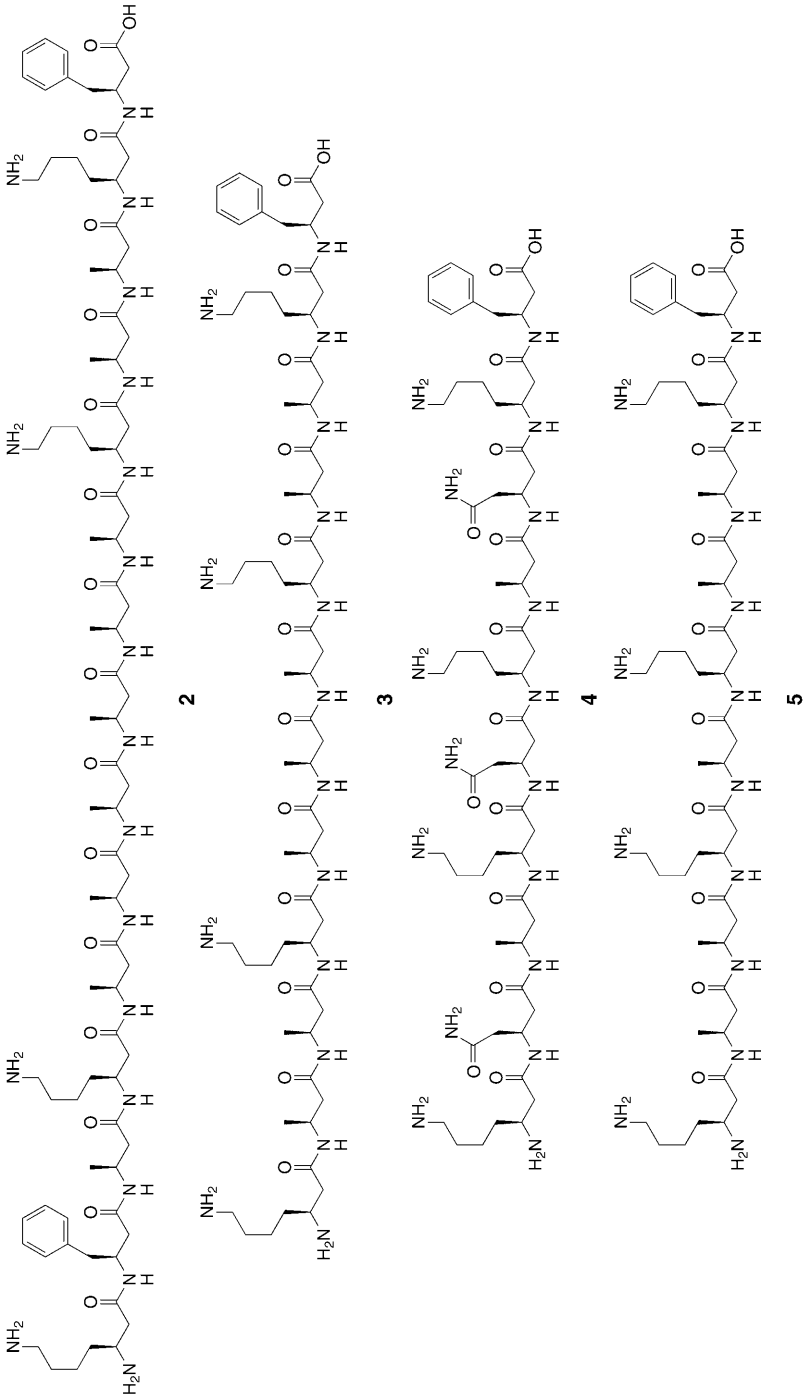
2
3
4
5

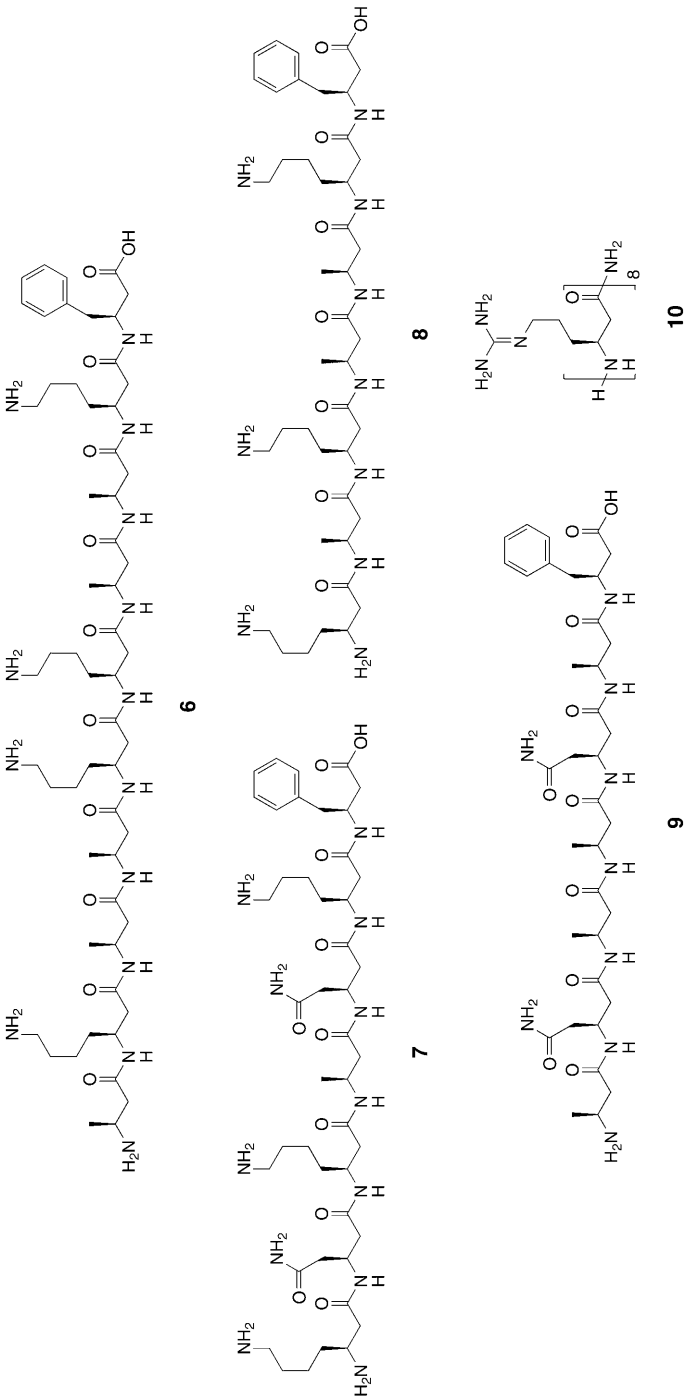
6
7
8
9
10

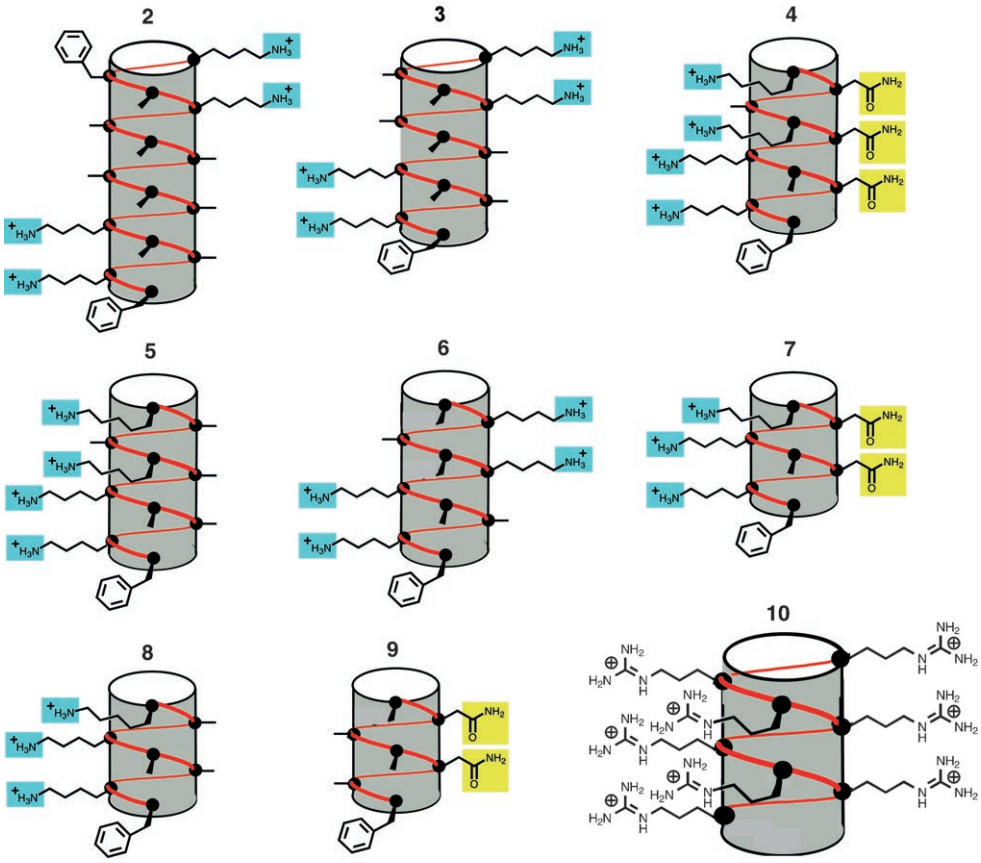

Fig. 2. *Schematic representations of helical structures of β^3-peptides* **2**–**10**

4. Spectroscopic Studies of β-Peptide Interactions with $dA_{20}dT_{20}$. – In our preliminary study [1], the CD signals from each oligonucleotide alone were subtracted from those of a mixture of **1** and the corresponding oligonucleotide so that any conformational changes of the peptide in the presence of the oligonucleotide (or conversely of the oligonucleotide in the presence of the peptide) would be detected. To judge the outcome of such CD studies in a more reliable and sensitive manner, CD titration of β-peptides against a $dA_{20}dT_{20}$ oligonucleotide was employed in the current study[8])[9]). Following common practice, CD spectra were measured at a range of peptide/oligonucleotide

---

[8]) Oligonucleotide $dG_{20}dC_{20}$ was not employed in the current study because it was suspected not to form a stable duplex under the experimental conditions. T_m Measurements of $dG_{20}dC_{20}$ did not give any clear melting temperature, indicating the malformation of duplex. Some publications suggest abnormality of duplex formation between oligoG and oligoC single strands [9].

[9]) Buffer solutions used in this study do not contain Mg^{2+}, which is commonly employed to stabilize the double helix.

ratios, which were scaled according to dilution factors, then subtracted by a likewise scaled pure oliogonucleotide signal, and finally overlaid (*Fig. 3*).

The observed progressive increase of *Cotton* effect at certain wavelengths along with the increase of peptide concentration was a clear indication of peptide–oligonucleotide interactions. Plotting the intensities of the *Cotton* effect (at positive maxima or negative minima) *vs.* peptide concentration revealed lines of steadily increasing intensity, without saturation. Of the ten β-peptides studied, the pentadecapeptides **1** and **2**, and β-octaarginine **10** showed significant interactions with the $dA_{20}dT_{20}$ DNA duplex, while there was little indication for interaction of dodecapeptide **3**, decapeptides **4**–**6**, and heptapeptides **7** and **8**: the CD curves of these β-peptides showed minimal deviation from the baseline, which suggests that there is essentially no interaction with $dA_{20}dT_{20}$[10]).

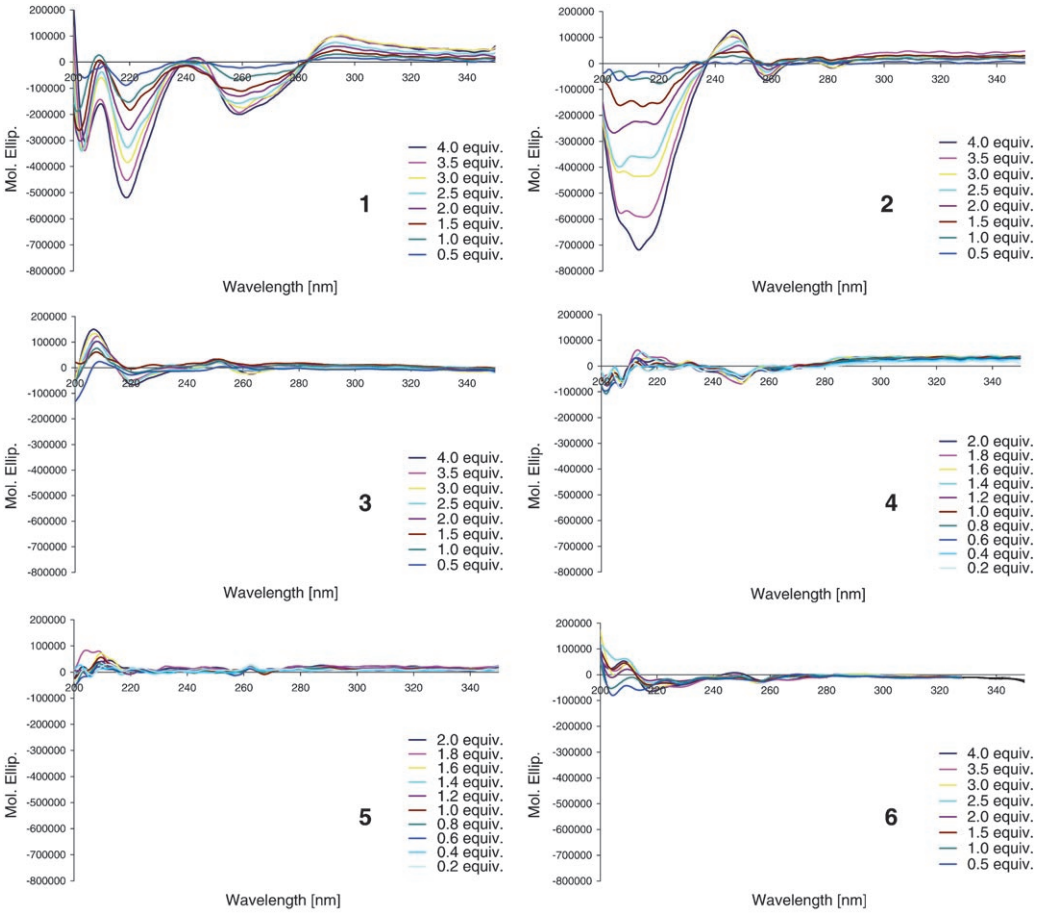

Fig. 3. *Non-normalized CD Spectra of β^3-peptides* **1**–**8** *and* **10** *titrated against a solution of $dA_{20}dT_{20}$ in aqueous buffer* (pH 7.5)

[10]) Peptide **9** was found to be insoluble in both H_2O and MeOH, and was, therefore, not included in the CD study.

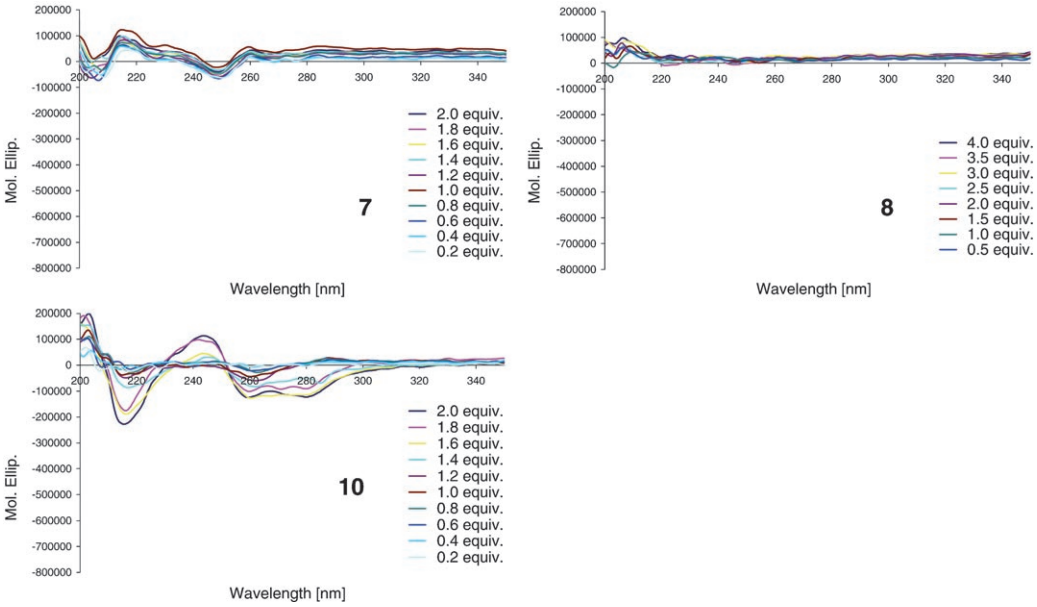

Fig. 3 (cont.)

Interestingly, pentadecapeptide **2** (lacking Asn side chains) showed strong interaction in the CD titration studies, albeit this interaction led to signals at different wavelengths, as compared to **1** (carrying Asn side chains); for **1**, minima were observed at 205, 220, and 260 nm, with a weak maximum at 290 nm and a zero-crossing point at 280 nm; for **2**, a weak minimum and a somewhat more intensive maximum were observed at *ca.* 260 and 250 nm, respectively, with a very intensive negative *Cotton* effect at 215 nm, and zero-crossing points at 235 and 250 nm. This indicates that the Asn residues are not critical for β-peptide–DNA interactions, but that the nature of the interaction may be different with and without the Asn side chains.

We attempted to further characterize the β-peptide–DNA interactions, and measured the degree of stabilization of the new conformations through the use of melting temperature (T_m) measurements. However, we were unsuccessful in obtaining clear-cut results. While reversibility/irreversibility of the duplex dissociation–association cycles was observed and was of itself an interesting finding, the obtained T_m values seemed to have no correlation with the CD studies[11])[12]). As such, the relevant T_m data are not included here.

5. Interactions of β-Peptide 1 with a CRE Consensus Site. – To investigate whether interactions of β-peptides with DNA duplexes could be demonstrated with a more com-

[11]) For melting curves obtained with $dA_{20}dT_{20}$ and peptide **1**, see [1].

[12]) A possible explanation could be that the peptide–oligonucleotide interaction is too weak to have an impact on the T_m of the duplex, although we hesitate to interpret the data as it is currently variable and inconclusive. Future studies are aimed at clarifying this issue.

plex DNA structure, we examined the CD spectra of β-peptides in the presence of a DNA duplex containing a cyclic-AMP response element (CRE), a sequence involved in the regulation of cAMP [10].

It is known that the factors that bind to CREs belong to a diverse family of basic leucine zipper (bZIP) transcriptional activators known as activating transcriptional factors (ATF) [11][12]. A well-known example is the transcriptional activator GCN4 (General Control Nonderepressable), a homodimeric protein that induces amino acid synthesis in yeast [13–16][13]). The DNA-binding region of the bZIP domain of GCN4 has the simplest known architecture among sequence-specific DNA-binding motifs (<25 amino acids) and consists of a C-terminal basic region that is largely disordered in the absence of DNA. Upon binding to DNA, the entire bZIP domain folds to a pair of α-helices that extend through the major groove of DNA at each recognition half site in a scissor-like fashion (*Fig. 4*) [18][19]. GCN4 has been shown to recognize the ATF/CREB[14]) site target sequence ATGACGTCAT [18][20][21], as well as the AP-1 site target sequence ATGACTCAT [15][19][22][23][15])[16]). Despite the two sites differing by a central GC base pair the binding affinities of GCN4 for the two recognition sites are very similar [25]. Although GCN4 was originally characterized as a positive regulator of genes expressed during amino acid starvation [13], it has since been shown to directly, or indirectly, regulate the expression of genes involved in purine biosynthesis, organelle biosynthesis, autophagy, glycogen homeostasis, and multiple stress responses [26][17]). In addition, the basic regions of a large number of bZIP proteins are closely related [19], and, in the case of proto-oncogenes *fos* and *jun*, completely homologous[15]).

Considering the importance of such DNA-binding proteins, any observed interactions of β-peptides with a CRE sequence, such as that recognized by GCN4, would be potentially interesting with regard to gene regulation. Therefore, pentadecamers **1** and **2**, and decamer **4** were titrated against a DNA-duplex 20-mer containing the ATF/CREB recognition sequence for GCN4 (*Fig. 4*).

Inspection of the corresponding CD curves clearly shows that there is an interaction, especially of the β-pentadecapeptide **1**, but also of **2**, with the ATF/CREB-containing DNA duplex, while lesser interaction is indicated for the decapeptide **4**. Interestingly, the CD spectrum for the titration of **1** with the ATF/CREB sequence showed negative *Cotton* effects at 220 and 265 nm, with zero crossing at 240 and 280 nm, and is very similar to that previously observed for the titration of **1** with $dA_{20}dT_{20}$ (*Fig. 3*). The CD curves of **2** titrated against the CRE sequence showed less pronounced negative

---

13) bZIP Factors bind as dimers to specific DNA recognitions sites and are believed to regulate the efficiency with which RNA polymerase II binds to DNA and initiates transcription [17].

14) ATF/CREB: activating transcription factor/cyclic-AMP responsive element binding proteins.

15) AP-1: activating protein 1. The AP-1 site is also recognized by the proto-oncogenes *fos* and *jun*, the basic region residues of which are homologous with that of GCN4, with absolute conservation of all the residues forming base-specific contacts [24].

16) The ATF/CREB site is a palindromic binding sequence (ATGAC), while the AP-1 site has a pseudo-palindromic sequence (ATGAC/G).

17) For an extensive list of genes putatively regulated by GCN4, and their respective sequences, see http://mips.gsf.de/proj/yeast/tables/uas/gcn4.html.

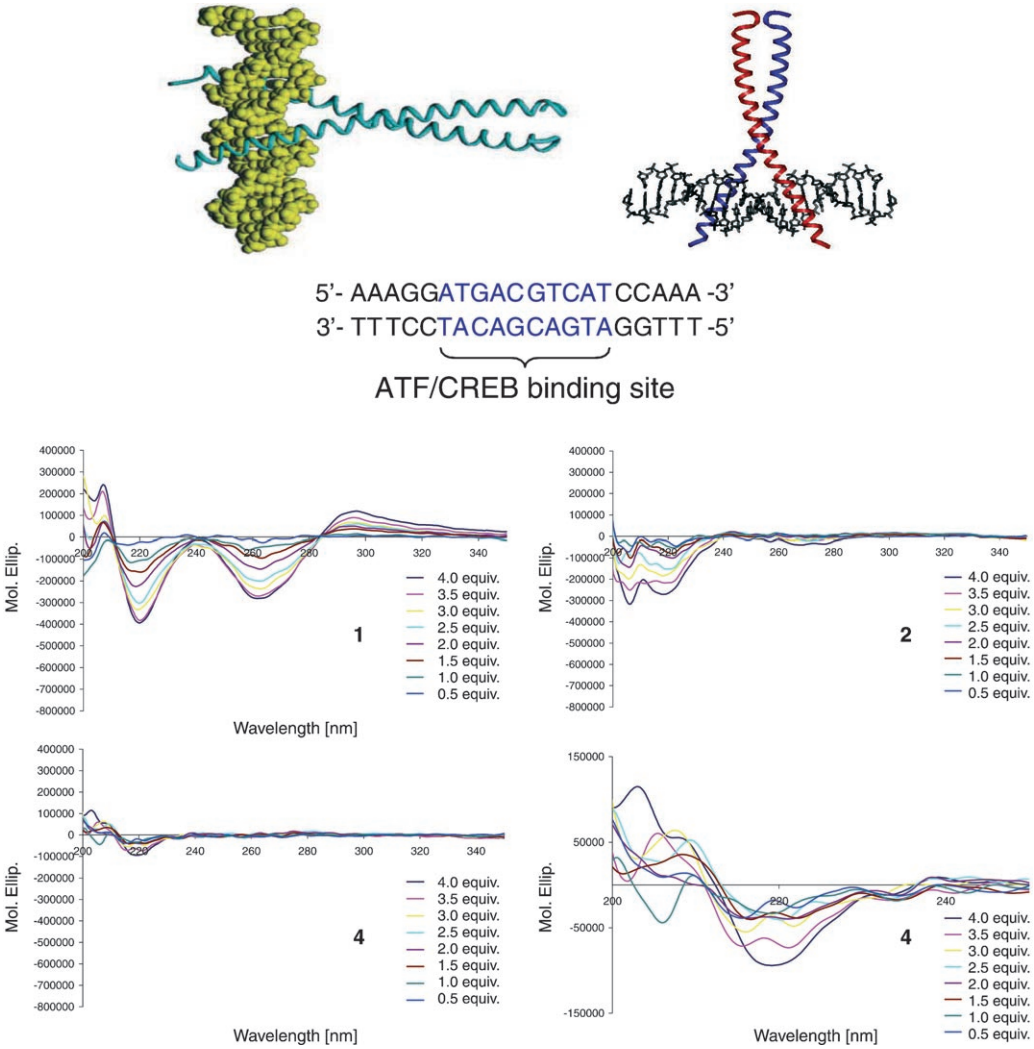

Fig. 4. Top: *Space-filling and stick models of GNC4-bZip binding to B-DNA*. Middle: *Duplex DNA 20-mer containing the ATF/CREB binding sequence for the regulatory protein GCN4* (shown in blue). Bottom: *Non-normalized CD spectra showing the interactions of* β^3*-peptides* **1**, **2**, *and* **4** *with the ATF/CREB sequence* (*Bottom right*: Note the expanded scales displayed for **4**).

Cotton effects at 205 and 220 nm. This is in contrast to the titration curves obtained with peptide **2** and $dA_{20}dT_{20}$ (*Fig. 3*), where a deep trough was observed at 215 nm. Obviously, β-pentadecapeptide **2** interacts differently with the two DNA duplexes. A blow-up of the CD spectrum of decapeptide **4** in the range of 200–240 nm is also shown in *Fig. 4*; the CD curve becomes more uniform as the number of equivalents of the peptide per DNA duplex increases.

6. Discussion. – When analyzing the CD curves obtained from the interaction of the studied β-peptides with DNA oligomers of $dA_{20}dT_{20}$ (*Fig. 3*) and a DNA-duplex 20-mer containing the ATF/CREB recognition sequence for GCN4 (*Fig. 4*), it is noticeable that, while the intensity of the curves increases with increasing concentration, no saturation limit was reached for any of the peptides. Possible reasons for this lack of saturation include: *i*) the range of peptide concentrations is too narrow, *ii*) the affinity of the peptide for the oligonucleotide is too low, *iii*) the peptide and oligonucleotide interactions are not limited to a 1:1 complex.

Of the ten peptides studied by CD difference analysis, pentadecapeptides **1** and **2**, and the octaarginine **10** significantly interacted with the oligonucleotides. Of these, all show a large negative *Cotton* effect at 220 nm, suggestive of a helical peptide structure[18]). Peptide **1** contains Asn side chains designed to interact with the DNA base pairs, and displays an additional negative *Cotton* effect at 260 nm when compared to **2**, which lacks Asn. However, **1** shows very similar CD curves in the presence of the two different DNA duplexes suggesting against peptide–base pair interactions as the major cause of complexation. On the other hand, peptide **2** shows differing CD patterns in the presence of the two different DNA duplexes. This implies that direct contact of base pairs with peptide side chains does exist, influencing complex formation *via* base pair–side chain interactions (the H-bonding properties of the base pairs A–T and G–C are shown in *Fig. 5*)[19]).

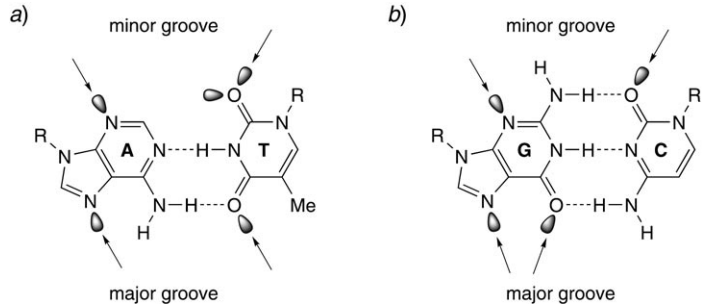

Fig. 5. *Schematic diagrams of the nucleotide bases A, T, G, and C in DNA.* Arrows mark the potential H-bond acceptor positions. *a*) Base pairing between adenine (**A**) and thymine (**T**). *b*) Base pairing between guanine (**G**) and cytosine (**C**).

It is apparent that a length dependency also exists for peptides **1**–**10** in order for peptide–DNA interactions to be observed: pentadecapeptides **1** and **2**, and octaarginine **10** show significant interaction, while peptides **3**–**9** show little interaction. However, all peptides contain cationic side chains (Lys or Arg) and, therefore, have an inherent affinity for negatively charged phosphate backbones. Whether this leads to conformationally distinct complex formation (thus observable by CD) might simply

[18]) We have also previously stated that CD curves are not always a reliable indication of structure [4][7b][27][28].

[19]) For an excellent review on the H-bonding properties of DNA, see [29].

depend on the alignment of such cationic side chains. The lack of observable interaction for peptides **3**–**9** may be simply due to their shorter peptide length and an improper alignment of Lys residues. Octaarginine **10** is unique in this regard, as it shows significant interaction with DNA duplexes despite its shorter length: this is presumably due to the strong salt-bridge and H-bond forming ability of the guanidinium groups on each side chain. The CD curve for the interaction of **10** with $dA_{20}dT_{20}$ also shows an additional negative *Cotton* effect at 280 nm that was not observed with the other peptides. It is of particular note that **10** is also known to intensively localize within the cellular nucleus of eukaryotic cells [6][7]. Therefore, it seems more natural to suggest that the proper alignment of Lys residues (this includes factors governed by peptide length) appears as the primary requirement for the observed DNA–peptide interactions, and that base pair–side chain interactions are not sufficient by themselves to bring the peptide and DNA together, even though this might have secondary contributions to the overall stability of the resulting complex. While the exact nature of the interactions between β-peptides and DNA is not yet known, the significance and sequence specificity of these interactions are under our utmost attention to address in the on-going studies.

7. Conclusions. – By CD analysis, we have further demonstrated that β-peptides can interact with DNA duplexes. In addition, we have shown for the first time an interaction of a β-peptide with a functional DNA sequence that is known to bind the regulatory protein GCN4. As our knowledge on the structural diversity of β-peptides and the requirements for small molecule–DNA binding increases, our ability to rationally design molecules leaps to improved control over specificity and selectivity of DNA–peptide binding. Given the unique properties of β-peptides and their stability towards proteolysis, this class of compound may offer yet further potential for applications within the realms of biomedical research.

We gratefully acknowledge continuing financial support of our research by *Novartis Pharma* and by the Swiss National Science Foundation. We thank the *New Zealand Foundation for Research Science and Technology* for a grant to *J. G.* Ms. *Brandenberg*'s help in measuring high-field NMR spectra is also appreciated.

Experimental Part

1. *General. Abbreviations.* DIPEA: Ethyldiisopropylamine (EtN(i-Pr)$_2$), DMAP: 4-(dimethylamino)pyridine, Fmoc: [(9*H*-fluoren-9-yl)methoxy]carbonyl, HATU: *O*-(7-azabenzotriazol-1-yl)-1,1,3,3-tetramethyluronium hexafluorophosphate, h.v.: high vacuum (0.01–0.1 Torr), MALDI: matrix-assisted laser desorption ionization, MeIm: 1-methyl-1*H*-imidazole, MSNT: 1-(mesitylene-2-sulfonyl)-3-nitro-1,2,4-triazole, TFA: trifluoroacetic acid (CF_3COOH), TNBS: 2,3,6-trinitrobenzenesulfonic acid.

All reagents were used as received from *Fluka*, *Aldrich*, or *Novabiochem*. Oligonucleotides were purchased from *Microsynth GmbH* (CH-Balgach). UV/VIS Spectra: *Perkin Elmer Lambda 40* photospectrometer. CD Spectra: *Jasco J-710* spectropolarimeter; from 195 to 250 nm at r.t. in 1-mm rectangular cells and subsequently normalized. NMR Spectra: *Bruker DRX-500* (^{1}H: 500 MHz) or *ARX-300* (^{1}H: 300 MHz); chemical shifts δ in ppm downfield from internal Me_4Si (= 0 ppm); *J* values in Hz. MS: *IonSpec Ultima 4.7-T-FT* ion cyclotron resonance (ICR, HR-MALDI, in 2,5-dihydroxybenzoic acid matrix) spectrometer; in *m*/*z* (% of basis peak). Lyophilization: *Hetosicc* cooling condenser with a h.v. pump. Buffer compositions (all solns. were sterilized in an autoclave prior to use): Buffer *A*: 1M phosphate buf-

fer (pH 7.5; 0.100 ml), 5M aq. NaCl soln. (40 µl), ultra-pure H_2O (4.860 ml). Buffer *B*: 1M Phosphate buffer (0.105 ml), 5M aq. NaCl soln. (42 µl), ultra-pure H_2O (4.853 ml). Buffer *C*: 1M phosphate buffer (0.101 ml), 5M aq. NaCl soln. (40 µl), ultra-pure H_2O (4.859 ml).

2. *Peptide Synthesis.* 2.1. *Anchoring of* N-*Fmoc-Protected Amino Acids on* Wang *Resin; Determination of Loading. General Procedure 1* (*GP 1*). Esterification of the Fmoc-protected amino acid with *Wang* resin was performed according to [8], by the MSNT/MeIm method. The resin was placed in a dry manual reactor, swollen in CH_2Cl_2 (20 ml/g resin) for 1 h, and washed with CH_2Cl_2. In a separate dry round-bottomed flask, equipped with a magnetic stirrer, the Fmoc-protected amino acid (5 equiv.) was dissolved in dry CH_2Cl_2 (3 ml/mmol), and MeIm (3.75 equiv.) and MSNT (5 equiv.) were added under Ar. Stirring was continued until all the MSNT dissolved. The yellow soln. was then added to the swollen resin, and the suspension was mixed by N_2 bubbling for 2–4 h. The resin was filtered, washed with CH_2Cl_2 (5 ml, 5×1 min), and dried under vacuum for 24 h. The resin substitution was determined by measuring the absorbance of the dibenzofulvene–piperidine adduct: two aliquots of the Fmoc-amino acid resin were weighed exactly (m_1(resin) and m_2(resin) [mg]) and suspended in an exact amount of piperidine soln. (20% in DMF) in volumetric flasks ($V_1 = V_2 = 10$ [ml]). After 30 min, the mixtures were transferred to a UV cell, and the absorbance (A) was measured relative to a blank piperidine soln. (20% in DMF). The concentrations (c_1 and c_2 [mM]) of the benzofulvene–piperidine adduct in soln. were determined using a calibration curve [8]. The loading (Subst.) was then calculated according to *Eqn. 1*:

$$\text{Subst}_n\ [\text{mmol/g resin}] = c_n \cdot V_n / \{m_n(\text{resin}) - [c_n \cdot V_n \cdot (M_r - 18)/1000]\} \quad (1)$$

(M_r = molecular weight of the Fmoc-protected amino acid).

The yield for the resin attachment (loading yield) was determined by *Eqn. 2*:

$$\text{Loading yield} = [(\text{Subst}_1 + \text{Subst}_2)/2]/\text{Subst}_{\text{theor.}} \quad (2)$$

2.2. *Capping. General Procedure 2* (*GP 2*). The peptide-resin was covered in DMF (2 ml), and the unreacted OH groups were capped by the addition of Ac_2O (10 equiv. in 1 ml of CH_2Cl_2) and DMAP (0.1 equiv. in 1 ml DMF), and mixing with N_2 bubbling for 1 h. The resin was washed with DMF (5 ml, 5×1 min).

2.3. *Deprotection of* N-*Fmoc-Protected Amino Acids on* Wang *Resin. General Procedure 3* (*GP 3*). The Fmoc deprotection was carried out with 20% piperidine in DMF (4 ml, 4×10 min) under N_2 bubbling. After filtration, the resin was washed with DMF (5 ml, 3×1 min) and CH_2Cl_2 (5 ml, 5×1 min).

2.4. *Coupling of β-Amino Acids on* Wang *Resin. General Procedure 4* (*GP 4*). The Fmoc deprotection was carried out according to *GP 3*. Solid-phase synthesis was continued by sequential incorporation of Fmoc-protected β-amino acids. For each coupling step, the resin was treated with a soln. of Fmoc-protected amino acid (3 equiv.), HATU (2.9 equiv.), and DIPEA (6 equiv.) in DMF (5 ml) for 1–2 h. Monitoring of the coupling reaction was performed with the TNBS test [30]. In case of a positive TNBS test (indicating incomplete coupling), the suspension was allowed to react for a further 1–2 h, or retreated with the same Fmoc-protected β-amino acid (2 equiv.) and coupling reagents. After complete coupling, the resin was washed with DMF (5 ml, 5×1 min) and CH_2Cl_2 (5 ml, 5×1 min). The cycle was then repeated until all remaining β-amino acids were incorporated.

2.5. Wang *Resin cleavage and Final Deprotection. General Procedure 5* (*GP 5*). The cleavage from the resin was performed according to [31]. The dry peptide-resin was suspended in a soln. of TFA/(i-Pr)$_3$SiH/H_2O (952 : 2.5 : 2.5, 10 ml) for 4 h. The resin was removed by filtration and washed with TFA (2×). The combined filtrate was diluted with CH_2Cl_2 (10 ml), and the volatiles were removed under reduced pressure. The resulting oily residue was treated with cold Et_2O to precipitate the crude peptide as the TFA salt.

2.6. *HPLC Analysis and Purification of β-Peptides.* RP-HPLC Analysis was performed using a *Macherey-Nagel* C_{18} column (*Nucleosil 100-5* C_{18} (250×4 mm)) by using a linear gradient of *A*: MeCN and *B*: 0.1% TFA in H_2O, at a flow rate of 1 ml/min with UV detection at 220 nm. Retention time

(t_R) in min. Aliquots of the crude products were purified by prep. RP-HPLC with a *Macherey-Nagel C_{18}* column (*Nucleosil 100-7 C_{18}* (250×21 mm)), using a gradient of *A* and *B* at a flow rate of 10 ml/min with UV detection at 220 nm, and then lyophilized to give 5–10 mg of each peptide (purity > 95%).

*H-(*S*)-β³hLys-(*S*)-β³hPhe-(*S*)-β³hAla-(*S*)-β³hLys-(*S*)-β³hGln-(*S*)-β³hAla-(*S*)-β³hAsn-(*S*)-β³hAla-(*S*)-β³hAla-(*S*)-β³hAsn-(*S*)-β³hLys-(*S*)-β³hAla-(*S*)-β³hAsn-(*S*)-β³hLys-(*S*)-β³hPhe-OH* (**1**). Fmoc-β³hPhe-OH (723 mg, 1.8 mmol) was loaded onto *Wang* resin according to *GP 1*. Loading was estimated as 0.72 mmol/g (80%) corresponding to 290 μmol of Fmoc-β³hPhe-OH. The resin was then capped according to *GP 2*, and the peptide synthesis was performed according to *GP 3* and *4*. Cleavage of the peptide from the resin according to *GP 5* gave the crude product **1**. Purification of an aliquot by prep. RP-HPLC (5–40% *A* in 50 min, 40–95% *A* in 20 min) and lyophilization yielded the TFA salt of **1** (7 mg). White solid. Anal. RP-HPLC (5–40% *A* in 50 min, 40–95% in 20 min): t_R 22.3, purity > 95%. ^{1}H-NMR (500 MHz, CD_3OD): 0.9–1.7 (*m*, 41 H); 2.02 (*m*, 2 H); 2.31–2.98 (*m*, 48 H); 3.56 (*m*, 1 H); 4.31–4.62 (*m*, 14 H); 7.22 (*m*, 10 H); 8.27 (*m*, 2 H); 8.53 (*m*, 9 H); 8.67 (*m*, 2 H). MALDI-MS: 1885.1 (19), 1884.1 (34), 1883.1 (29, $[M+Na]^+$), 1864.1 (22), 1863.1 (59), 1862.1 (100, $[M+2\,H]^+$), 1861.1 (90, $[M+H]^+$), 1848.1 (13), 1847.1 (17), 1846.1 (16), 1845.1 (28), 1844.1 (26), 1763.0 (19), 1762.0 (37), 1761.0 (39). HR-MS: 1861.1430 ($[M+H]^+$, $C_{89}H_{150}N_{23}O_{20}^+$; calc. 1861.1427).

*H-(*S*)-β³hLys-(*S*)-β³hPhe-(*S*)-β³hAla-(*S*)-β³hLys-(*S*)-β³hAla-(*S*)-β³hAla-(*S*)-β³hAla-(*S*)-β³hAla-(*S*)-β³hAla-(*S*)-β³hLys-(*S*)-β³hAla-(*S*)-β³hAla-(*S*)-β³hLys-(*S*)-β³hPhe-OH* (**2**): Fmoc-β³hPhe-OH (362 mg, 0.9 mmol) was loaded onto *Wang* resin according to *GP 1*. Loading was estimated as 0.675 mmol/g (75%) corresponding to 135 μmol of Fmoc-β³hPhe-OH. The resin was then capped according to *GP 2*, and the peptide synthesis was performed according to *GP 3* and *4*. Cleavage of the peptide from the resin according to *GP 5* gave the crude product **2**. Purification of an aliquot by preparative RP-HPLC (5–50% *A* in 50 min) and lyophilization yielded **2** as a white solid. Anal. RP-HPLC (5% *A* for 5 min, 5–50% *A* in 30 min): t_R 26.7, purity > 98%. ^{1}H-NMR (500 MHz, CD_3OD): 1.16–1.28 (*m*, 27 H); 1.29–1.76 (*m*, 24 H); 2.30–2.99 (*m*, 50 H); 3.57 (*m*, 1 H); 4.29–4.66 (*m*, 13 H); 4.75 (*m*, 1 H); 7.18–7.29 (*m*, 10 H); 7.55 (*d*, *J* = 8.2, 1 H); 7.71 (*d*, *J* = 9.5, 1 H); 8.16 (*d*, *J* = 8.9, 1 H); 8.19 (*d*, *J* = 9.1, 1 H); 8.40–8.54 (*m*, 6 H); 8.58 (*d*, *J* = 8.8, 1 H); 8.67 (*d*, *J* = 8.6, 1 H). MALDI-MS: 1699.1 (13), 1698.1 (26, $[M+Na]^+$), 1697.1 (26), 1678.1 (15), 1677.1 (48), 1676.1 (100, $[M+H]^+$), 1675.1 (92, M^+), 1659.1 (13), 1658.1 (13), 1578.0 (12), 1577.0 (37), 1576.0 (79), 1575.0 (71). HR-MS: 1675.1039 (M^+, $C_{84}H_{144}N_{19}O_{16}^+$; calc. 1675.1038).

*H-(*S*)-β³hLys-(*S*)-β³hAla-(*S*)-β³hAla-(*S*)-β³hLys-(*S*)-β³hAla-(*S*)-β³hAla-(*S*)-β³hAla-(*S*)-β³hLys-(*S*)-β³hAla-(*S*)-β³hAla-(*S*)-β³hLys-(*S*)-β³hPhe-OH* (**3**): Fmoc-β³hPhe-OH (605 mg, 1.51 mmol) was loaded onto *Wang* resin according to *GP 1*. Loading was estimated as 0.54 mmol/g (60%) corresponding to 181 μmol of Fmoc-β³hPhe-OH. The resin was then capped according to *GP 2*, and the peptide synthesis was performed according to *GP 3* and *4*. Cleavage of the peptide from the resin according to *GP 5* gave the crude product **3**. Purification by prep. RP-HPLC (5–50% *A* in 50 min) and lyophilization yielded **3** as a white solid. Anal. RP-HPLC (5% *A* for 5 min, 5–50% *A* in 30 min): t_R 20.5, purity > 98%. ^{1}H-NMR (300 MHz, CD_3OD): 1.19 (*m*, 24 H); 1.29–1.81 (*m*, 24 H); 2.32–3.01 (*m*, 32 H); 3.64 (*m*, 1 H); 4.34–4.60 (*m*, 11 H); 7.23 (*m*, 5 H); 7.70 (*m*, 2 H); 8.15 (*m*, 2 H); 8.41 (*m*, 5 H); 8.61 (*d*, *J* = 8.0, 1 H). ESI-MS: 1343.9 (4, $[M+H]^+$), 693.0 (15), 692.5 (10), 684.0 (13), 683.5 (79), 673.0 (60), 672.5 (83, $[M+2\,H]^{2+}$), 449.3 (26), 448.9 (77), 448.6 (100, $[M+3\,H]^{3+}$). HR-MS: 672.4615 ($[M+2\,H]^{2+}$, $C_{66}H_{120}N_{16}O_{13}^{2+}$; calc. 672.4610). HR-MS: 1342.9064 (M^+, $C_{66}H_{118}N_{16}O_{13}^+$; calc. 1342.9064).

*H-(*S*)-β³hLys-(*S*)-β³hAsn-(*S*)-β³hAla-(*S*)-β³hLys-(*S*)-β³hAsn-(*S*)-β³hLys-(*S*)-β³hAla-(*S*)-β³hAsn-(*S*)-β³hLys-(*S*)-β³hPhe-OH* (**4**). Fmoc-β³hPhe-OH (181 mg, 0.45 mmol) was loaded onto *Wang* resin according to *GP 1*. Loading was estimated as 0.69 mmol/g (76%) corresponding to 67.5 μmol of Fmoc-β³hPhe-OH. The resin was then capped according to *GP 2*, and the peptide synthesis was performed according to *GP 3* and *4*. Cleavage of the peptide from the resin according to *GP 5* gave the crude product **4**. Purification of an aliquot by prep. RP-HPLC (5–50% *A* in 50 min) and lyophilization yielded **4** as a white solid. Anal. RP-HPLC (5% *A* for 5min, 5–50% *A* in 30 min): t_R 16.9, purity > 98%. ^{1}H-NMR (500 MHz, CD_3OD): 1.19 (*d*, *J* = 6.6, 3 H); 1.23 (*d*, *J* = 6.6, 3 H); 1.29–1.83 (*m*, 24 H); 2.30–3.00 (*m*, 46 H); 3.65 (*m*, 1 H); 4.35–4.59 (*m*, 8 H); 7.18–7.27 (*m*, 5 H); 7.65 (*d*, *J* = 8.9, 1 H); 7.78 (*d*, *J* = 8.8, 1 H); 8.19 (*d*, *J* = 8.7, 1 H); 8.26 (*d*, *J* = 9.1, 1 H); 8.41 (*d*, *J* = 9.1, 1 H); 8.47 (*d*, *J* = 9.4, 1 H); 8.60 (*d*, *J* = 8.6, 1 H).

MALDI-MS: 1347.8 (15), 1346.8 (22), 1326.8 (15), 1325.8 (36), 1324.8 (48, $[M+Na]^+$), 1304.8 (29), 1303.8 (75), 1302.8 (100, $[M+H]^+$), 1286.8 (17), 1285.8 (22), 1203.7 (21), 1202.7 (31). HR-MS: 1302.8248 ($[M+H]^+$, $C_{61}H_{108}N_{17}O_{14}^+$; calc. 1302.8262).

*H-(*S*)-β³hLys-(*S*)-β³hAla-(*S*)-β³hAla-(*S*)-β³hLys-(*S*)-β³hAla-(*S*)-β³hLys-(*S*)-β³hAla-(*S*)-β³hAla-(*S*)-β³hLys-(*S*)-β³hPhe-OH* (**5**). Fmoc-β³hPhe-OH (181 mg, 0.45 mmol) was loaded onto *Wang* resin according to *GP 1*. Loading was estimated as 0.69 mmol/g (76%) corresponding to 67.5 μmol of Fmoc-β³hPhe-OH. The resin was then capped according to *GP 2*, and the peptide synthesis was performed according to *GP 3* and *4*. Cleavage of the peptide from the resin according to *GP 5* gave the crude product **5**. Purification of an aliquot by prep. RP-HPLC (5–50% *A* in 50 min) and lyophilization yielded **5** as a white solid. Anal. RP-HPLC (5% *A* for 5min, 5–50% *A* in 30 min): t_R 17.5, purity > 98%. ^{1}H-NMR (300 MHz, CD_3OD): 1.18 (*m*, 15 H); 1.29–1.81 (*m*, 24 H); 2.32–3.00 (*m*, 30 H); 3.63 (*m*, 1 H); 4.33–4.54 (*m*, 9 H); 7.21 (*m*, 5 H); 7.71 (*m*, 2 H); 8.16 (*m*, 2 H); 8.34 (*m*, 2 H); 8.50 (*d*, *J* = 9.0, 1 H). MALDI-MS: 1196.8 (21), 1195.8 (29, $[M+Na]^+$), 1175.8 (26), 1174.8 (71), 1173.8 (100, $[M+H]^+$), 1156.8 (13), 1074.7 (30), 1073.7 (46). HR-MS: 1173.8070 (M^+, $C_{58}H_{105}N_{14}O_{11}^+$; calc. 1173.8087).

*H-(*S*)-β³hAla-(*S*)-β³hLys-(*S*)-β³hAla-(*S*)-β³hAla-(*S*)-β³hLys-(*S*)-β³hLys-(*S*)-β³hAla-(*S*)-β³hAla-(*S*)-β³hLys-(*S*)-β³hPhe-OH* (**6**). Fmoc-β³hPhe-OH (181 mg, 0.45 mmol) was loaded onto *Wang* resin according to *GP 1*. Loading was estimated as 0.66 mmol/g (75%) corresponding to 66 μmol of Fmoc-β³hPhe-OH. The resin was then capped according to *GP 2*, and the peptide synthesis was performed according to *GP 3* and *4*. Cleavage of the peptide from the resin according to *GP 5* gave the crude product **6**. Purification of an aliquot by prep. RP-HPLC (5–50% *A* in 50 min) and lyophilization yielded **6** as a white solid. Anal. RP-HPLC (5% *A* for 5 min, 5–50% *A* in 30 min): t_R 18.1, purity > 98%. ^{1}H-NMR (500 MHz, CD_3OD): 1.14–1.23 (*m*, 12 H); 1.31–1.79 (*m*, 24 H); 1.42 (*d*, *J* = 6.7, 3 H); 2.31–2.96 (*m*, 30 H); 3.76 (*m*, 1 H); 4.32 (*m*, 2 H); 4.40–4.57 (*m*, 7 H); 7.22 (*m*, 5 H); 7.72 (*m*, 1 H); 7.98 (*m*, 1 H); 8.15 (*m*, 3 H); 8.31 (*m*, 1 H); 8.51 (*m*, 2 H). MALDI-MS: 1196.8 (22), 1195.8 (31, $[M+Na]^+$), 1175.8 (26), 1174.8 (71), 1173.8 (100, $[M+H]^+$), 1157.8 (16), 1156.8 (24), 1132.8 (13), 1131.8 (36), 1130.8 (55). HR-MS: 1173.8103 ($[M+H]^+$, $C_{58}H_{105}N_{14}O_{11}^+$; calc. 1173.8087).

*H-(*S*)-β³hLys-(*S*)-β³hAsn-(*S*)-β³hLys-(*S*)-β³hAla-(*S*)-β³hAsn-(*S*)-β³hLys-(*S*)-β³hPhe*-OH (**7**). Fmoc-β³hPhe-OH (181 mg, 0.45 mmol) was loaded onto *Wang* resin according to *GP 1*. Loading was estimated as 0.69 mmol/g (76%) corresponding to 67.5 μmol of Fmoc-β³hPhe-OH. The resin was then capped according to *GP 2*, and the peptide synthesis was performed according to *GP 3* and *4*. Cleavage of the peptide from the resin according to *GP 5* gave the crude product **7**. Purification of an aliquot by prep. RP-HPLC (5–50% *A* in 50 min) and lyophilization yielded **7** as a white solid. Anal. RP-HPLC (5% *A* for 5 min, 5–50% *A* in 30 min): t_R 15.0, purity > 98%. ^{1}H-NMR (CD_3OD, 300 MHz): 1.19 (*d*, *J* = 6.7, 3 H); 1.25–1.83 (*m*, 18 H); 2.27–3.01 (*m*, 26 H); 3.62 (*m*, 1 H); 4.30 (*m*, 3 H); 4.53 (*m*, 1 H); 7.22 (*m*, 5 H); 7.78 (*m*, 2 H); 7.91 (*d*, *J* = 9.1, 1 H); 8.16 (*d*, *J* = 9.1, 1 H); 8.25 (*d*, *J* = 8.7, 1 H). MALDI-MS: 992.6 (19), 991.6 (36), 971.6 (13), 970.6 (39), 969.6 (71, $[M+Na]^+$), 949.6 (17), 948.6 (54), 947.6 (100, $[M+H]^+$), 931.6 (13), 930.6 (22), 848.5 (13), 847.5 (27). HR-MS: 947.6029 ($[M^+$, $C_{45}H_{79}N_{12}O_{10}^+$; calc. 947.6042).

*H-(*S*)-β³hLys-(*S*)-β³hAla-(*S*)-β³hLys-(*S*)-β³hAla-(*S*)-β³hAla-(*S*)-β³hLys-(*S*)-β³hPhe-OH* (**8**). Fmoc-β³hPhe-OH (181 mg, 0.45 mmol) was loaded onto *Wang* resin according to *GP 1*. Loading was estimated as 0.69 mmol/g (76%) corresponding to 67.5 μmol of Fmoc-β³hPhe-OH. The resin was then capped according to *GP 2*, and the peptide synthesis was performed according to *GP 3* and *4*. Cleavage of the peptide from the resin according to *GP 5* gave the crude product **8**. Purification of an aliquot by prep. RP-HPLC (5–50% *A* in 50 min) and lyophilization yielded **8** as a white solid. Anal. RP-HPLC (5% *A* for 5 min, 5–50% *A* in 30 min): t_R 16.0, purity > 98%. ^{1}H-NMR (300 MHz, CD_3OD): 1.17 (*m*, 9 H); 1.29–1.79 (*m*, 18 H); 2.27–2.99 (*m*, 22 H); 3.61 (*m*, 1 H); 4.23–4.51 (*m*, 6 H); 7.19 (*m*, 5 H); 7.79 (*m*, 3 H); 8.14 (*m*, 1 H). MALDI-MS: 906.6 (29), 905.6 (56), 885.6 (14), 884.6 (50), 883.6 (99, $[M+Na]^+$), 863.6 (10), 862.6 (36), 861.6 (70, $[M+H]^+$), 844.6 (16), 762.5 (13), 761.5 (13), 475.2 (26). HR-MS: 861.5939 ($[M+H]^+$, $C_{43}H_{77}N_{10}O_8^+$; calc. 861.5926).

*H-(*S*)-β³hAla-(*S*)-β³hAsn-(*S*)-β³hAla-(*S*)-β³hAla-(*S*)-β³hAsn-(*S*)-β³hAla-(*S*)-β³hPhe-OH* (**9**). Fmoc-β³hPhe-OH (181 mg, 0.45 mmol) was loaded onto *Wang* resin according to *GP 1*. Loading was estimated as 0.69 mmol/g (76%) corresponding to 67.5 μmol of Fmoc-β³hPhe-OH. The resin was then capped according to *GP 2*, and the peptide synthesis was performed according to *GP 3* and *4*. Cleavage of the

peptide from the resin according to *GP 5* gave the crude product **9**. Purification of an aliquot by prep. RP-HPLC (5–50% *A* in 50 min) and lyophilization yielded **9** as a white solid. Anal. RP-HPLC (5% *A* for 5 min, 5–50% *A* in 30 min): t_R 20.1, purity > 98%. MALDI-MS: 799.4 (18), 798.4 (45, $[M+Na]^+$), 777.4 (42), 776.4 (100, $[M+H]^+$). HR-MS: 776.4310 ($[M+H]^+$, $C_{36}H_{58}N_9O_{10}^+$; calc. 776.4607).

H-((S)-β³hArg)₈-NH₂ (**10**). Prepared according to our previously published method [5].

3. *CD Titration.* 3.1. *Single-Strand Oligonucleotide Annealing. General Procedure 6* (*GP 6*). Each single-strand oligonucleotide was dissolved in sterilized ultra-pure H_2O with the final concentration of 1 mM. A pair of single-strand oligonucleotide solns. (100 µl, 1 mM) were mixed in a PCR tube, which was placed in a PCR machine (*MJ Research PTC-200*) for annealing (heated to 99° over *ca.* 3 min then slowly cooled to 3° at −1°/min) to yield a 0.5 mM soln. of a double-strand oligonucleotide.

3.2. *CD Titration of Double-Strand Oligonucleotides with β-Peptides. General Procedure 7* (*GP 7*). In a quartz-glass CD cell (1-mm optical path, *ca.* 450-µl volume with *Teflon* cap) was placed an aliquot of the 0.5 mM double-strand oligonucleotide soln. (16 µl, 8 nmol), to which buffer *B* (334 µl) was added, and the whole soln. (total volume 350 µl) was mixed well by turning the cell up side down several times. The cell was mounted on the CD spectrometer (stabilized for 30 min), and the sample temp. was equilibrated at 10°, followed by a CD measurement (λ range: 190–350 nm, data pitch 0.5 nm, band width 1 nm, response 0.5 s, scan speed 20 nm/min, 5 scans). After the first measurement, the cell was taken out of the sample chamber, and a 0.4 mM soln. of β-peptide in buffer *A* (10 µl, 4 nmol) was added to the cell. The whole soln. (total volume 360 µl) was mixed well, and the cell was mounted again to the CD spectrometer. After temp. equilibration, the second CD spectrum was measured under the identical conditions as above. Addition of the β-peptide and CD measurements were repeated a further seven times (in total, 4.0 equiv. of β-peptide was added to each double-strand oligonucleotide). The CD signals from each measurement were converted to molecular ellipticity based on the concentrations of the double-strand oligonucleotide and overlaid for comparison.

REFERENCES

[1] T. Kimmerlin, K. Namoto, D. Seebach, *Helv. Chim. Acta* **2003**, *86*, 2104.
[2] 'Protein Structure and Function', G. A. Petsko, and D. Ringe, New Science Press, London, 2004.
[3] 'Nucleic Acids in Chemistry and Biology', Eds., G. M. Blackburn, M. J. Gait, Oxford University Press Inc., New York, 1996.
[4] J. Gardiner, A. V. Thomae, R. I. Mathad, D. Seebach, S. D. Krämer, *Chem. Biodiv.* **2006**, *3*, 1181; T. Hitz, R. Iten, J. Gardiner, K. Namoto, P. Walde, D. Seebach, *Biochemistry* **2006**, *45*, 5817.
[5] D. Seebach, K. Namoto, Y. R. Mahajan, P. Bindschädler, R. Sustmann, M. Kirsch, N. S. Ryder, M. Weiss, M. Sauer, C. Roth, S. Werner, H.-D. Beer, C. Mundling, P. Walde, M. Voser, *Chem. Biodiv.* **2004**, *1*, 65; M. Rueping, Y. Mahajan, M. Sauer, D. Seebach, *ChemBioChem* **2002**, *3*, 257.
[6] B. Geueke, K. Namoto, I. Agarkova, J.-C. Perriard, H.-P. Kohler, D. Seebach, *ChemBioChem* **2005**, *6*, 982.
[7] a) D. Seebach, T. Kimmerlin, R. Sebesta, M. A. Campo, A. K. Beck, *Tetrahedron* **2004**, *60*, 7455; b) D. Seebach, A. K. Beck, D. J. Bierbaum, *Chem. Biodiv.* **2004**, *1*, 1111.
[8] 'Fmoc Solid Phase Peptide Synthesis: A Practical Approach', Vol. 222, Eds. W. C. Chang, and P. D. White, Oxford University Press, Oxford, 2000.
[9] U. Dornberger, M. Leijon, H. Fritzsche, *J. Biol. Chem.* **1999**, *274*, 6957.
[10] R. Yaar, L. M. Cataldo, A. Tzatsos, C. E. Francis, Z. Zhao, K. Ravid, *Mol. Pharmacol.* **2002**, *62*, 1167.
[11] K. K. Yamamoto, G. A. Gonzales, P. Menzel, J. Rivier, M. R. Montminy, *Cell* **1990**, *60*, 611.
[12] W. H. Landshulz, P. F. Johnson, S. L. McKnight, *Science* **1988**, *240*, 1759.
[13] D. E. Hill, I. A. Hope, J. P. Macke, K. Struhl, *Science* **1986**, *234*, 451.
[14] I. A. Hope, K. Struhl, *EMBO* **1987**, *6*, 2781.
[15] T. Alber, *Current Biol.* **1993**, *3*, 182.
[16] E. K. O'Shea, J. D. Klemm, P. S. Kim, T. Alber, *Science* **1991**, *254*, 539.
[17] A. D. Baxevanis, C. R. Vinson, *Curr. Opin. Genet. Dev.* **1993**, *3*, 278.
[18] W. Keller, P. König, T. J. Richmond, *J. Mol. Biol.* **1995**, *254*, 657.

[19] T. E. Ellenberger, C. J. Brandl, K. Struhl, S. C. Harrison, *Cell* **1992**, *71*, 1223.
[20] C. Berger, I. Jelesarov, H. R. Bossard, *Biochemistry* **1996**, *35*, 14984.
[21] T. W. Hai, F. Liu, W. J. Coukos, M. R. Green, *Genes Dev.* **1989**, *3*, 2083.
[22] K. Arndt, G. R. Fink, *Proc. Natl. Acad. Sci. U.S.A.* **1986**, *83*, 8516.
[23] A. R. Oliphant, C. J. Brandl, K. Struhl, *Mol. Cell. Biol.* **1989**, *9*, 2944.
[24] K. Struhl, *Cell* **1987**, *50*, 841.
[25] J. W. Sellers, A. C. Vincent, K. Struhl, *Mol. Cell. Biol.* **1990**, *10*, 5077.
[26] K. Natarajan, M. R. Meyer, B. M. Jackson, D. Slade, C. Roberts, A. G. Hinnebusch, M. Marton. *Mol. Cell. Biol.* **2001**, *13*, 4347.
[27] D. Seebach, J. Schreiber, P. I. Arvidsson, J. Frackenpohl, *Helv. Chim. Acta* **2001**, *84*, 271.
[28] A. Glattli, X. Daura, D. Seebach, W. F. van Gunsteren, *J. Am. Chem. Soc.* **2002**, *124*, 12972.
[29] P. Dervan, *Top. Curr. Chem.* **2005**, *253*, 1.
[30] W. S. Hancock, J. E. Battersby, *Anal. Biochem.* **1976**, *71*, 260.
[31] *Novabiochem* 2002/3 catalogue: The Fine Art of Solid Phase Synthesis.

Received October 19, 2006